J. Phycol. **45,** 413–426 (2009)

DOI: 10.1111/j.1529-8817.2009.00648.x

UNRAVELING THE REGULATION OF NITROGEN ASSIMILATION IN THE MARINE DIATOM *THALASSIOSIRA PSEUDONANA* (BACILLARIOPHYCEAE): DIURNAL VARIATIONS IN TRANSCRIPT LEVELS FOR FIVE GENES INVOLVED IN NITROGEN ASSIMILATION[1]

Kathryn L. Brown, Katrina I. Twing[3]*, and Deborah L. Robertson*[2]

Biology Department, Clark University, 950 Main Street, Worcester, Massachusetts 01610, USA

We examined the diurnal expression of five genes encoding nitrogen-assimilating enzymes in the marine diatom *Thalassiosira pseudonana* (Hust.) Hasle et Heimdal following a transition from NH_4^+- to NO_3^--supplemented media. The accumulation of *nia* transcripts (encoding nitrate reductase, NR) following the transition to NO_3^--supplemented media was similar to previously reported changes in NR abundance and activity. *Nia* mRNA levels varied diurnally, and the diurnal oscillations were abolished when cells were transferred to continuous light. Genes encoding chloroplastic (*nii*A) and cytosolic (*nir*B) nitrite reductases were identified in the genome of *T. pseudonana*. *Nii*A and *nir*B transcript levels increased within 2 h following the addition of NO_3^- and varied diurnally. Patterns of diurnal variation in *nia*, *nii*A, and *gln*II (encoding the chloroplast-localized glutamine synthetase) mRNA abundances were similar. *Nir*B and *gln*N (encoding the cytosolic-localized glutamine synthetase) mRNA levels also oscillated diurnally; however, the oscillation was out of phase with *nia*, *nii*A, and *gln*II. We propose that NO_3^- is assimilated into organic molecules in both the chloroplast and cytosol of diatoms and that enzymes encoded by *nir*B and *gln*N contribute to the ecologically important dark assimilation of NO_3^- observed in marine diatoms. As with *nia*, the diurnal variations in *nii*A, *nir*B, *gln*II, and *gln*N were abolished when cells were transferred to continuous light. Our results demonstrate that transcript accumulation is not circadian controlled, but, rather, changes in metabolic pools triggered by light:dark (L:D) transitions may be important in regulating the cellular mRNA levels encoding these key nitrogen assimilating enzymes.

Key index words: **diatoms; gene expression; glutamine synthetase; nitrate reductase; nitrite reductase; nitrogen assimilation; quantitative real-time PCR**

Abbreviations: C_t, **cycle threshold; Fd, ferredoxin; GS, glutamine synthetase; L:D, light:dark; L:L, continuous light; NR, nitrate reductase; NiR, nitrite reductase; QRT-PCR, quantitative reverse-transcriptase PCR**

The assimilation of inorganic nitrogen into organic compounds is a key process regulating the growth and productivity of photosynthetic eukaryotes and requires coordinated expression and regulation of enzymes in the cytosol, chloroplast, and mitochondria (Turpin 1991, Lea 1993, Hodges 2002). Knowledge of the molecular and cellular regulation of these enzymes is critical to understanding the metabolic response of photosynthetic eukaryotes to environmental variations in nitrogen, temperature, and light, and thus the regulation of primary productivity. Although there have been numerous studies of the coordinated regulation of genes involved in nitrogen assimilation in vascular plants (Lam et al. 1996, Wang et al. 2000, Stitt et al. 2002, Foyer et al. 2003, Scheible et al. 2004), there is limited information concerning the molecular regulation of nitrogen assimilation in other lineages of photosynthetic eukaryotes.

Nitrogen availability in marine ecosystems varies over several spatial and temporal scales. For example, in highly productive coastal upwelling systems, wind-driven pulses of nutrient-rich water periodically enhance the local productivity of phytoplankton populations, which are most often dominated by diatoms (Kudela et al. 1997, Kudela and Dugdale 2000, Wilkerson et al. 2000, Bruland et al. 2005). As upwelling relaxes and the supply of nitrate decreases, or as nitrogen is regenerated through biological activity, phytoplankton may persist by using internal nutrient stores or regenerated forms of nitrogen such as ammonium, urea, and other sources of dissolved organic nitrogen (DON) (Dortch et al. 1984, Dickson and Wheeler 1995, Bode et al. 1997).

As a result of its importance in the regulation of primary productivity and vertical carbon flux, the regulation of NO_3^- uptake and assimilation has

[1]Received 26 September 2007. Accepted 13 October 2008.
[3]Present address: University of Delaware, College of Marine and Earth Sciences, 700 Pilottown Road, Lewes, Delaware 19958, USA.
[2]Author for correspondence: e-mail debrobertson@clarku.edu.

been the focus of numerous studies (Dortch 1990, Smith et al. 1992, Berges and Harrison 1995, Berges et al. 1995, Vergara et al. 1998, Hildenbrand and Dahlin 2000, Jochem et al. 2000, Hildebrand 2005). Following the active uptake of NO_3^- from extracellular sources, NO_3^- is reduced to NO_2^- by the activity of a NADH-dependent nitrate reductase (NR). Nitrite reductase (NiR) catalyzes the reduction of NO_2^- to NH_4^+, which is assimilated into the amino acid glutamine via the coordinated activities of glutamine synthetase (GS) and glutamate synthase (GOGAT). The assimilation of NO_3^- is energetically costly, and, as observed in vascular plants, green algae, and fungi, NR expression in diatoms is regulated at multiple levels. Transcription of *nia* (the gene encoding NR) occurs in the presence of NO_3^- and is reduced, or inhibited, by NH_4^+ (Parker and Armbrust 2005, Poulsen and Kroger 2005, Poulsen et al. 2006). In *T. pseudonana*, *nia* transcript abundance increased in response to high levels of irradiance and cold temperatures, indicating that NO_3^- reduction can, under certain conditions, contribute to the dissipation of excess energy (Lomas and Glibert 1999a,b, Parker and Armbrust 2005).

NR abundance and activity are also regulated posttranscriptionally in diatoms. Using *nia* promoter and terminator elements, Poulsen et al. (2006) demonstrated that NO_3^- is required for the translation of *nia* in N-starved cultures of *Cylindrotheca fusiformis* and *T. pseudonana*. Furthermore, although the posttranslational mechanisms are yet to be elucidated, NR abundance and activity vary diurnally, are enhanced by NO_3^- and light, and are repressed by NH_4^+ in many species of diatoms and natural assemblages of phytoplankton (Smith et al. 1992, Berges et al. 1995, Vergara et al. 1998, Jochem et al. 2000).

Fewer studies have examined the regulation of enzymes downstream of NR or those involved with assimilation of other nitrogen sources, such as ammonium, urea, or DON (Zehr and Falkowski 1988, Robertson and Alberte 1996, Robertson et al. 1999, Milligan and Harrison 2000, Takabayashi et al. 2004, Hildebrand 2005). As observed in vascular plants and green algae, diatoms express a chloroplast-targeted ferredoxin-dependent nitrite reductase (Fd-NiR) and glutamine synthetase (GSII), which are involved in the assimilation of NO_2^- produced from NO_3^- (Robertson et al. 1999, Milligan and Harrison 2000, Armbrust et al. 2004, Takabayashi et al. 2004, Parker and Armbrust 2005). Fd-NiR is a metaloprotein containing a siroheme and a 4Fe–4S iron:sulfur cluster and catalyzes the six-electron reduction of NO_2^- to NH_4^+. In photosynthetic organisms, the physiological electron donor is ferredoxin, which is reduced by light-dependent electron transport in chloroplasts (Wray 1993, Swamy et al. 2005). The reduction in photosynthetic electron flow to ferredoxin in iron-limited diatom cells may limit NO_3^- assimilation in iron-limited regions of the oceans (Milligan and Harrison 2000).

GS catalyzes the ATP-dependent formation of glutamine via the condensation of NH_4^+ and glutamate. *Gln*II mRNA (encoding GSII) levels were higher in NO_3^--supplemented *T. pseudonana* and *Skeletonema costatum* cultures than in NH_4^+-supplemented cultures, implicating GSII in the assimilation of NH_4^+ produced from NO_3^--reduction (Armbrust et al. 2004, Takabayashi et al. 2004). *Gln*II levels also increased under enhanced photorespiratory conditions, suggesting that GSII is also involved in the assimilation of photorespiratory produced NH_4^+ (Parker and Armbrust 2005).

The expression of multiple GS isoenzymes that are compartmentalized in the cytosol or chloroplast is a common characteristic of eukaryotic photoautotrophs. Diatoms, in contrast to vascular plants and some green algae, express enzymes from two distinct GS gene families: the chloroplast-targeted enzyme GSII (*gln*II) discussed above and a cytosolic-localized GSIII (encoded by *gln*N). GSIII is expressed in *S. costatum* cells grown with either NH_4^+- or NO_3^--supplemented media (Robertson and Alberte 1996), suggesting that the enzyme may be involved with the primary assimilation of both NH_4^+ and NO_3^-, the assimilation of NH_4^+ produced via photorespiration, and anaplerotic reactions involving amino acid biosynthesis and nitrogen mobilization.

Our understanding of the metabolic capacity of marine diatoms has been greatly advanced by the sequencing of diatom genomes (Armbrust et al. 2004). One surprise to emerge from the diatom genome data was the presence of a gene encoding a cytosolic-localized NAD(P)H-dependent nitrite reductase (NAD(P)H-NiR) homologous to *nir*B genes in fungi and bacteria (Armbrust et al. 2004, Allen et al. 2006). Bacterial and fungal *nir*B holoenzymes are homodimers with FAD- and NAD(P)H-dependent functions at the N-terminal end of the protein and NO_2^--reducing functions near the C-terminus (Colandene and Garrett 1996). The enzymes contain a well-conserved iron–sulfur half domain (2Fe–2S), a nitrite/sulfite reductase ferredoxin-like half domain, and binding sites for two prosthetic groups: iron–sulfur (4Fe–4S) and siroheme (Colandene and Garrett 1996, Olmo-Mira et al. 2006). Homologs of NAD(P)H-NiR have not been identified in plant or green algal genome projects, and thus its presence in the diatom genome suggests a pathway for nitrogen assimilation that, in terms of photoautotrophs, appears unique to diatoms.

Nitrate is not only a major nutrient for vascular plants, but also acts as a signal triggering rapid changes in pathway-specific and global changes in gene expression (Stitt 1999, Wang et al. 2000, Stitt et al. 2002, Foyer et al. 2003, Scheible et al. 2004, Blasing et al. 2005). For example, the addition of NO_3^- induces the expression of genes involved in NO_3^- uptake, primary assimilation (nitrate transporters, *nia*, *nii*A, and chloroplast-targeted GS), the

production of organic acids and reducing equivalents and triggers changes in developmental pathways (Scheible et al. 2004). In several species of vascular plants, both nitrate and light are required for high levels of NR expression, and posttranslational regulatory processes are overlaid onto the circadian control of gene expression (Lillo et al. 2001, Blasing et al. 2005).

Less is known regarding the regulation and coordinated changes in the expression of genes involved in nitrogen assimilation in diatoms. Therefore, in this study, we examined diurnal changes in the expression of genes known or predicted to be involved in the assimilation of NO_3^- in *T. pseudonana* following a transition in nitrogen availability. We used quantitative reverse-transcriptase PCR (QRT–PCR) to measure transcript levels of five enzymes (*nia*, *nii*A, *nir*B, *gln*II, and *gln*N) and used the coordinated patterns of mRNA accumulation to infer the physiological functions of the enzymes. We determined that the mRNA levels for the five genes varied diurnally and that the diurnal changes in transcript levels were abolished under constant light conditions. Our results suggest that transcript accumulation is not circadian controlled, but rather, changes in metabolic pools triggered by L:D transitions appear important in regulating the accumulation of mRNA encoding these five nitrogen assimilating enzymes.

MATERIALS AND METHODS

Identification of genes involved with nitrogen assimilation. Gene and mRNA sequences for five enzymes involved in nitrogen assimilation were retrieved from the publically available *T. pseudonana* genome project (http://genome.jgi-psf.org/Thaps3/Thaps3.home.html). The identities of the genes were confirmed by BLASTP comparisons with sequences in GenBank (Altschul et al. 1997). The genes selected were *nia* (nitrate reductase), *nii*A (ferredoxin dependent nitrite reductase), *nir*B (NADPH-dependent nitrite reductase), *gln*II (glutamine synthetase-type II), and *gln*N (glutamine synthetase-type III). The gene nomenclature used in this article reflects the homology between the *T. pseudonana* genes and genes previously characterized in other organisms.

*Nii*A and *nir*B have not been well characterized in diatoms, and therefore the predicted protein structures of the two enzymes were further explored in this study. Homologous sequences were retrieved from GenBank using BlastP (Altschul et al. 1997) and aligned using ClustalW (Thompson et al. 1994) with default settings. Protein structure predictions of the two enzymes were obtained using the PhyloFacts (Krishnamurthy et al. 2006) and Conserved Domain Database (Marchler-Baue et al. 2007) software programs. Putative N-terminal signal peptides and chloroplast transit sequences were predicted using TargetP v1.1 and ChloroP v1.1 (Nielsen et al. 1997, Emanuelsson et al. 1999, 2000) and were evaluated based on diatom-specific transit peptide characteristics presented by Gruber et al. (2007).

Culture information. T. pseudonana (CCMP1335) was obtained from the Provosoli-Guillard National Center for Culture of Marine Phytoplankton (Boothbay Harbor, ME, USA) and maintained axenically on f/2-supplemented sterile seawater (Guillard and Ryther 1962, Guillard 1975). Cultures were grown at 17°C on a 12:12 L:D cycle and were illuminated ($135 \pm 6\ \mu E \cdot m^{-2} \cdot s^{-1}$) from above and along one side using cool-white lights. Cell densities were measured daily using a hemacytometer. For all experiments, cells were grown on f/2-enriched natural seawater media made from a single collection of seawater. Cells were collected by vacuum filtration onto sterile 0.45 μM HA membrane filters (Millipore, Billerica, MA, USA) and immediately frozen in liquid nitrogen.

Diel expression of nitrogen assimilation genes following a transition in nitrogen availability. A repeated measures experimental design was used to examine the diurnal variation in the accumulation of *nia*, *nii*A, *nir*B, *gln*II, and *gln*N (Table 1) transcripts in *T. pseudonana* following a transition from NH_4^+- to NO_3^--supplemented f/2 media.

Culture conditions and sampling: Three replicate cultures (3 L) of *T. pseudonana* were started with a 1:1,000 dilution of an axenically maintained stock culture and were grown at 17°C on a 12:12 L:D cycle for 10 d. NH_4^+ (60 μM NH_4Cl final concentration) was the sole nitrogen source added to the f/2-enriched natural seawater media and was added to the culture media on days 1, 5, 8, 9, and 10. Since NH_4^+ is a known phytotoxin, the scheduled additions maintained the NH_4^+ concentration below 100 μM while allowing for increases in biomass. Ammonium was depleted by the cells over the course of 24 h on days 7–10 (data not shown). Cells were collected beginning on the 11th day following the initiation of the culture and were collected on three consecutive days at seven time points during each day (0700, 0900 [start of the light period], 1100, 1300, 1500, 1800, and 2100 h [end of the light period]). On day 11 at 0700 h ($t = -2$ h), 100 mL of cells were collected from each replicate culture by vacuum filtration and care was taken not to expose cultures or cells to light. At 0900 h ($t = 0$ h), cultures were transferred into three 5 L carboys containing 2.5 L of sterile f/2-enriched natural seawater containing $NaNO_3$ at a final concentration of 880 μM. Following the nutrient shift, cells from 200 mL of media were collected by filtration.

Nutrient analysis: During the 10 d growth period, prior to the transfer to NO_3^--enriched f/2 media, 1.5 mL samples of culture media were collected from each replicate culture for analysis for NH_4^+ concentration. The samples were centrifuged at 13,000*g* for 3 min at room temperature. The resulting pellet was discarded and remaining seawater was frozen at −20°C for later analysis. The concentration of NH_4^+ in the culture media was measured using standard colorimetric protocols (Parsons et al. 1984) and commercially available reagents (Sigma Diagnostics, St. Louis, MO, USA). NO_3^- concentration was determined colorimetrically using the spongy cadmium method (Jones 1984, Gao 1997). Standards of known concentration ranging between 0 and 25 μM $NaNO_2$ were prepared daily and were treated in the same manner as samples. Standards, ranging between 0 and 25 μM $NaNO_3$, were used to confirm the effectiveness of the cadmium reduction. For both assays, the absorbances of triplicate 200 μL aliquots of each sample were measured spectrophotometrically using a Lambda Scan 200 × 96-well microplate reader (MWG-BioTech, High Point, NC, USA; Hernandez-Lopez and Vargas-Albores 2003).

Preparation of nucleic acids—RNA and cDNA: RNA was extracted using an RNeasy® kit (Qiagen Inc., Valencia, CA, USA) following the manufacturer's protocol, with the following modifications. Cells were washed from membrane filters with 1.2 mL of extraction buffer RLT from the RNeasy® kit and transferred to 2.0 mL tubes containing RNase-free 0.5 mm zirconia/silica beads that had been presoaked in 0.5 mL of RLT. Cells were lysed by beating for 2 min using a bead mill (MiniBeadBeater™, BioSpec Products Inc., Barklesville, OK, USA), and the lysate was clarified by centrifugation for 4 min at 13,000*g* at room temperature. The supernatant was transferred to a 15 mL round-bottom test tube, and an equal volume of 70% ethanol was added and mixed. All subsequent RNA preparation steps followed the manufacturer's instructions.

TABLE 1. Oligonucleotide primers used in quantitative reverse-transcriptase PCR (QRT–PCR) analyses of *Thalassiosira pseudonana* gene expression. Sequences for the forward and reverse primer for each gene are presented as well as the final concentration of each primer in the QRT–PCR reaction. The protein ID and chromosomal location of each gene were based on the information provided for the *T. pseudonana* genome (http://genome.jgi-psf.org/Thaps3/Thaps3.home.html). The region amplified indicates the position of the primers relative to the start of the open reading frame. The final concentration (Conc.) of each primer in the QRT–PCR reaction is presented.

Gene	Protein or enzyme	Protein ID	Chromosome	Region amplified	Sequence	Conc. (nM)
β-actin	A	139154	20	794–1120	5′-AGC CCA ACC TTA CTG GAT TGG AGA-3′ 5′-TGT GAA CAA TCG AAG GTC CCG ACT-3′	100
nia	NR	110642	16	1851–2007	5′-GAT CTT CAT CCT GGT GGA GCT G-3′ 5′-CAT CAG AAA CAA CCG CCA CTG-3′	100
nirB	NAD(P)H-NiR	26941	2	372–494	5′-CCA TTT GTT CCA CCC ATT CCT G-3′ 5′-GAT AAC GGC AGC ACT CTT GAC G-3′	100
niiA	Fd-NiR	262125	4	1086–1407	5′-ATC AGC AAA GGA GTG CCG TG-3′ 5′-TCC AGT CCA GTG AAT ACG AAT CG-3′	150
glnII	GSII	26051	22	1103–1247	5′-TGA GGA TTG GAA GGG ATA CCG-3′ 5′-AGG GCA CTG ATT TCT GGA ACG-3′	100
*gln*N	GSIII	270138	24	1784–2008	5′-AAG GAG GCA CTC GGA GAG ATT C-3′ 5′-CTC GTC AAA GTA GGT TGG CTC G-3′	100

RNA concentration was determined spectrophotometrically by measuring the absorbance at 260 and 280 nm in an MWG-BioTech Lambda Scan 200 × 96-well microplate reader with KCJunior Software (MWG-BioTech). The conversion factor of an absorbance of 1 unit at 260 nm corresponding to 40 $\mu g \cdot mL^{-1}$ of RNA was used to determine RNA quantity using path length corrected absorbance values. The purity of each RNA sample was evaluated by the ratio of the absorbance values at 260 and 280 nm (A_{260}/A_{280}). RNA was stored at −80°C.

cDNA was generated from 1 μg of RNA using QuantiTect® Reverse Transcription kit (Qiagen Inc.) following the manufacturer's protocol. Genomic DNA was eliminated by incubating samples at 42°C for 2 min in gDNA Wipeout Buffer (Qiagen Inc.). The reverse transcription reaction components were added following manufacturer's instructions and allowed to incubate for 30 min at 42°C and then 3 min at 95°C. Resulting cDNA was stored at −20°C. Control reactions lacking reverse transcriptase were used to confirm the absence of genomic DNA.

QRT–PCR: cDNA was amplified using the Full Velocity™ SYBR® Green QPCR kit (Stratagene, La Jolla, CA, USA) following the manufacturer's protocol and using ROX (6-carboxyl-X-rhodamine) as the reference dye. A 1:10 dilution of previously generated cDNA was used for each sample. Sequences of the gene-specific primers used in this study are provided in Table 1 and were derived from sequences obtained from the *T. pseudonana* genome project (http://genome.jgi-psf.org/Thaps3/Thaps3.home.html). Primer concentrations were optimized for each gene-specific primer-pair to yield PCR efficiencies between 90% and 110% as recommended by the manufacturer (Stratagene). To avoid amplification of potentially contaminating genomic DNA, the forward primer for *nia* spanned the fourth exon-exon splice junction and therefore did not amplify *nia* genomic DNA. The forward and reverse primers for *nirB, gln*II, and *gln*N anneal to sequences in exons separated by at least one intron; PCR products produced from the amplification of genomic DNA would therefore be larger than products from cDNA and detected in dissociation curves (see below).

For each sample, PCR reactions were performed in triplicate in a 96-well Mx3000P™ thermocycler (Stratagene) in a total volume of 25 μL. No-template controls were included with each plate. The following cycle parameters were used for all QRT-PCR runs: 10 min at 95°C, 40 cycles of 95°C for 30 s, 55°C for 1 min, and 72°C for 30 s. The dissociation profile was generated by heating samples at 95°C for 1 min, annealing at 55°C, and then heating using a stepwise linear increase in temperature ending at 95°C; SYBR green fluorescence was recorded during the linear increase in temperature. The sizes of PCR products were confirmed using 3% Nusieve® GTG® Agarose (Cambrex Bio Science, Rockland, ME, USA) in Tris–Acetate–EDTA buffer (0.04 M Tris–acetate; 1 mM EDTA, pH 8; Sambrook and Russell 2001).

Cycle threshold (C_t) values were determined for the replicate PCR reactions using the default setting in MxPro Software (Stratagene). C_t-values for each gene of interest were normalized to β-actin levels using the double reciprocal method (Luu-The et al. 2005). Briefly, for every sample, the C_t-value of the gene of interest was divided by the C_t-value for actin. The ratio was multiplied by the grand mean of all actin C_t's for a given treatment. The fold change in mRNA levels was calculated for each gene as the difference between the normalized C_t at any given time point and the C_t at $t = 0$ h (Livak and Schmittgen 2001).

Patterns of mRNA accumulation in response to L:D cycles and continuous irradiance: A single factor, repeated measures experimental design was used to determine whether the diel patterns of *nia*, *nii*A, *nir*B, *gln*II, and *gln*N mRNA accumulation in *T. pseudonana* were circadian regulated.

Culture conditions and sampling: Six replicate 5 L cultures of *T. pseudonana* were started on f/2-enriched natural seawater media from a 1:100 dilution of a 1 L axenically maintained stock culture that had been grown on 12:12 L:D cycle for 8 d. On the third day (72 h) following initiation of the cultures, three randomly selected replicate cultures were shifted to continuous light (L:L), while the other three replicate cultures continued on the 12:12 L:D cycle. Irradiance level for cultures experiencing L:L conditions was 72.71 ± 8.57 $\mu E \cdot m^{-2} \cdot s^{-1}$, while irradiance during the light period of the L:D condition was 80.43 ± 8.62 $\mu E \cdot m^{-2} \cdot s^{-1}$.

Cells were collected by filtration (as described previously) over a 3 d period. For the first sampling day, cells from 200 mL of each culture were collected by filtration at 0700, 0900 (start of the light period), 1100, 1300, 1500, 1800, and 2100 h (end of the light period). For the remaining 2 d, cells from 100 mL of culture media were collected.

Experimental analyses: NO_3^- concentration was determined as described above for all samples using 1.5 mL of each culture, which was centrifuged at 13,000*g* for 3 min at room temperature. The resulting pellet was discarded and remaining seawater was frozen at −20°C for later analysis. RNA extraction, cDNA synthesis, and QRT–PCR were performed and analyzed as described previously.

Statistical analyses: Results from all experiments were analyzed using the JMP® 6 statistical software package (SAS Institute Inc., Cary, NC, USA). Homogeneity of sample variances was evaluated using Levine's test. A two-way analysis of variance (ANOVA) with repeated measures on one factor was used to test for differences in transcript levels in cultures grown on L:D or L:L using the multivariate analysis of variance (MANOVA) model (Lehman et al. 2005). Correlations between transcript levels were evaluated using the Person product-moment correlation. Values are presented as means ± 1 standard error, unless otherwise noted.

RESULTS

*Diurnal variation in the accumulation of mRNA for five nitrogen assimilating enzymes. Nia, nii*A, *nir*B, *gln*II, and *gln*N transcript levels were normalized to β-actin mRNA levels. C_t-values for β-actin ranged between 18 and 31 (indicating higher and lower abundance of β-actin cDNA in the sample, respectively), similar to the range observed for the genes of interest. The abundance of β-actin mRNA did not vary significantly over the course of the experiment ($F_{14,40}$ = 1.4302; P = 0.1675).

To investigate the diurnal patterns of mRNA accumulation, three replicate cultures were grown for 10 d with NH_4^+ as the sole added nitrogen source, reaching a final cell density of $\sim 10^6$ cells · mL^{-1} (Fig. 1). On day 11, cultures were transferred to new carboys containing an equal volume of f/2 media; the decrease in cell density in Figure 1 represents this dilution. Following the transition to improved growth conditions, the concentration of NO_3^- remained above 700 μM for the duration of the experiment (data not shown).

Nitrate reductase. Nia mRNA abundance increased steadily during the first light period following the transfer of cells to NO_3^--enriched medium and was ~20 times greater at the onset of the second light period (Fig. 2A) than at the time of the transition to new media (0 h). The diurnal variation in *nia* accumulation was similar on the second and third day of sampling (24–60 h); transcript abundance was high at the onset of the light phase (24 and 48 h) and subsequently declined throughout the light period.

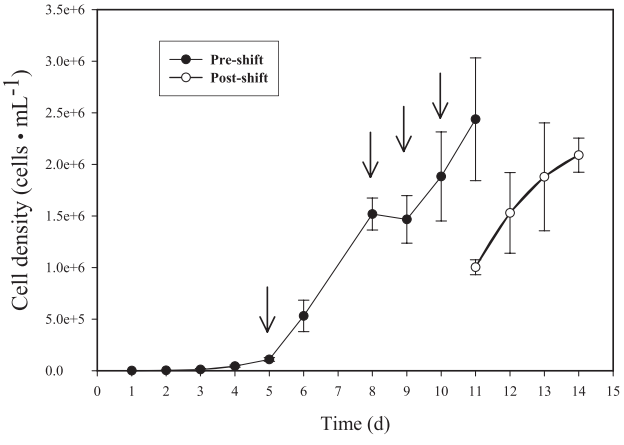

FIG. 1. Changes in *Thalassiosira pseudonana* cell density prior to and following a transition to NO_3^--supplemented f/2 media. Cells were grown on 12:12 light:dark (L:D) cycle. Prior to day 11, cultures were supplemented with 60 μM NH_4^+ (final concentration) on days 1, 5, 8, 9, and 10. On day 11, cells were transferred to f/2-supplemented natural seawater media containing 880 μM NO_3^- (open circles). Following the transition on day 11, symbols represent mean ± 1 SD from three replicate cultures.

Nitrite reductases. The annotated amino acid sequence of *T. pseudonana* Fd-NiR that was obtained from publicly available genome data (http://genome.jgi-psf.org/Thaps3/Thaps3.home.html) lacked a portion of the N-terminus, which we identified as the most 5′, in-frame start codon (ATG). The complete predicted open reading frame was 605 amino acids and shared homology with Fd-NiR (encoded by *nii*A) from cyanobacteria, green algae, and vascular plants, with the greatest similarity observed between sequences of the diatom and that of the chlorarachniophyte *Bigelowiella natans* (51% identity, E = $3e^{-157}$, Fig. 3). Both signal and transit peptides were identified in the diatom Fd-NIR sequence using TargetP v1.1 and ChloroP v1.1, respectively (Nielsen et al. 1997, Emanuelsson et al. 1999, 2000). The predicated cleavage site for the signal peptide was identified between amino acids 27 and 28 and was similar to the sequence logos proposed by Gruber et al. (2007); the predicted cleavage of the transit peptide was between amino acids 48 and 49. Chloroplast transit sequences were also predicted in the Fd-NiR sequences of the other photosynthetic eukaryotes presented in Figure 3. These results are consistent with the prediction that the Fd-NiR enzyme functions in the chloroplast.

Fd-NiRs are monomeric enzymes, and two well-conserved nitrite/sulfite ferredoxin-like half domains and two nitrite/sulfite reductase 4Fe–4S domains were identified in the predicted diatom sequence (Fig. 3). Several potentially charged residues in the N-terminal region of the enzyme, which may be involved in the stabilization of the siroheme, nitrite binding, and electron transfer (Swamy et al. 2005), were well conserved among the aligned sequences. In addition, four, well-conserved cysteines near the C-terminus, which coordinate the Fe–S cluster (Swamy et al. 2005), were identified.

*Nii*A transcript levels increased at the onset of the first light period following the transition to the NO_3^--enriched medium and remained relatively constant during the first 6 h of the light period before decreasing (Fig. 2B). On the second and third days of the experiment, *nii*A transcript levels were ~100 times higher at the onset of the light period (24 and 48 h, respectively) than at the transition to new media (0 h) and declined toward the end of the light period. There was a positive correlation between *nii*A and *nia* levels (r = 0.6408; t = 3.683; P = 0.0017), indicating that the diurnal variation in the transcript accumulation was similar for the two genes.

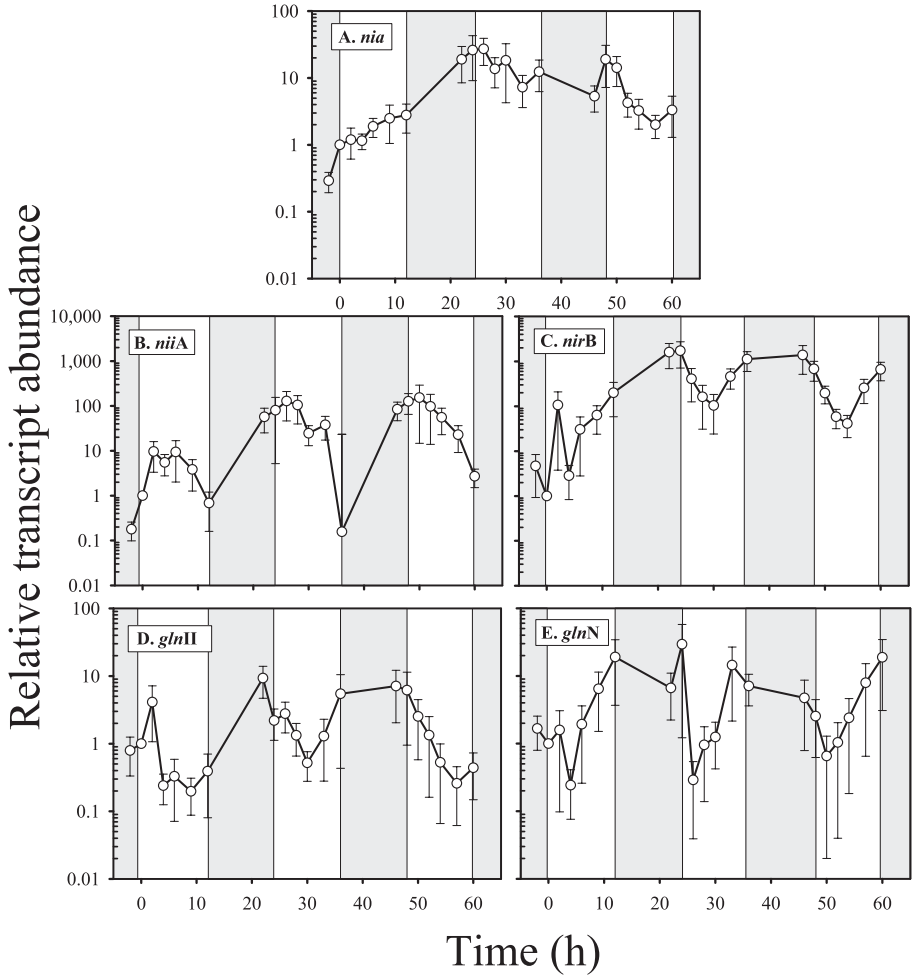

FIG. 2. Changes in relative transcript abundance for *nia* (NR; A), *nii*A (Fd-dependent NiR; B), *nir*B (NAD(P)H-dependent NiR; C), *gln*II (GSII; D), and *gln*N (GSIII; E) in *Thalassiosira pseudonana*. Relative transcript abundances were calculated as described in Materials and Methods and normalized to levels measured at $t = 0$ h. Shaded bars represent the dark period of a 12:12 light:dark (L:D) cycle. Time (h) is represented relative to the time that cells were transferred to f/2-supplemented natural seawater containing 880 μM NO_3^- (0 h). In all panels, symbols represent mean and ± 1 SE from three replicate cultures.

As with *nii*A, the annotated amino acid sequence for the *T. pseudonana* NAD(P)H-NiR obtained from the publically available database (http://genome.jgi-psf.org/Thaps3/Thaps3.home.html) lacked a portion of the N-terminus, as indicated by the presence of an upstream, in-frame start codon. The complete predicted open reading frame of the *T. pseudonana* NAD(P)H-dependent NiR was 1126 amino acids and homologous to *nir*B genes described from bacteria and fungi (52% identical to NAD(P)H-NiR from *Planctomyces maris*, E ≈ 0; Fig. 4). Bacterial and fungal *nir*B holoenzymes are homodimers characterized as having FAD- and NAD(P)H-dependent functions at the N-terminal end of the enzyme with nitrite-reducing functions near the C-terminus (Colandene and Garrett 1996). A predicted, well-conserved pyridine nucleotide-disulfide oxidoreductase domain was identified in the N-terminal region of the NAD(P)H-NiR alignment, which is predicted to bind FAD and pyridine nucleotides (Krishnamurthy et al. 2006). A bacterioferritin-associated ferredoxin-like iron–sulfur half domain (2Fe–2S) was also identified and contained five conserved cysteine residues in our alignment; the two most proximal and two most distal cysteine residues are involved in the coordination of two Fe ions (Garg et al. 1996). As observed in Fd-NiR, a nitrite/sulfite reductase ferredoxin-like half domain and a nitrite and sulfite reductase 4Fe–4S domain were observed toward the C-terminal end of the enzyme. In addition, a region homologous to the *nir*D Rieske domain was observed near the C-terminus. Within this domain, two conserved cysteine residues are involved in the coordination of one Fe ion, while two conserved histadine residues coordinate a second Fe ion. This region is necessary for NADH-NiR activity and is encoded by a separate gene in *Escherichia coli* but is fused to the *nas*B gene (encoding the bacterial assimilatory nitrate reductase) in other bacteria and fungi (Colandene and Garrett 1996).

Analysis of the N-terminal sequence of the *T. pseudonana* NAD(P)H-NiR was ambiguous in terms of identifying the cellular location of the enzyme. A N-terminal signal and chloroplast transit peptide (cleavage sites were predicted at amino acids 21 and 42, respectively) were identified in TargetP v1.1 and ChloroP v1.1 (Nielsen et al. 1997, Emanuelsson et al. 2000); however, the predicted

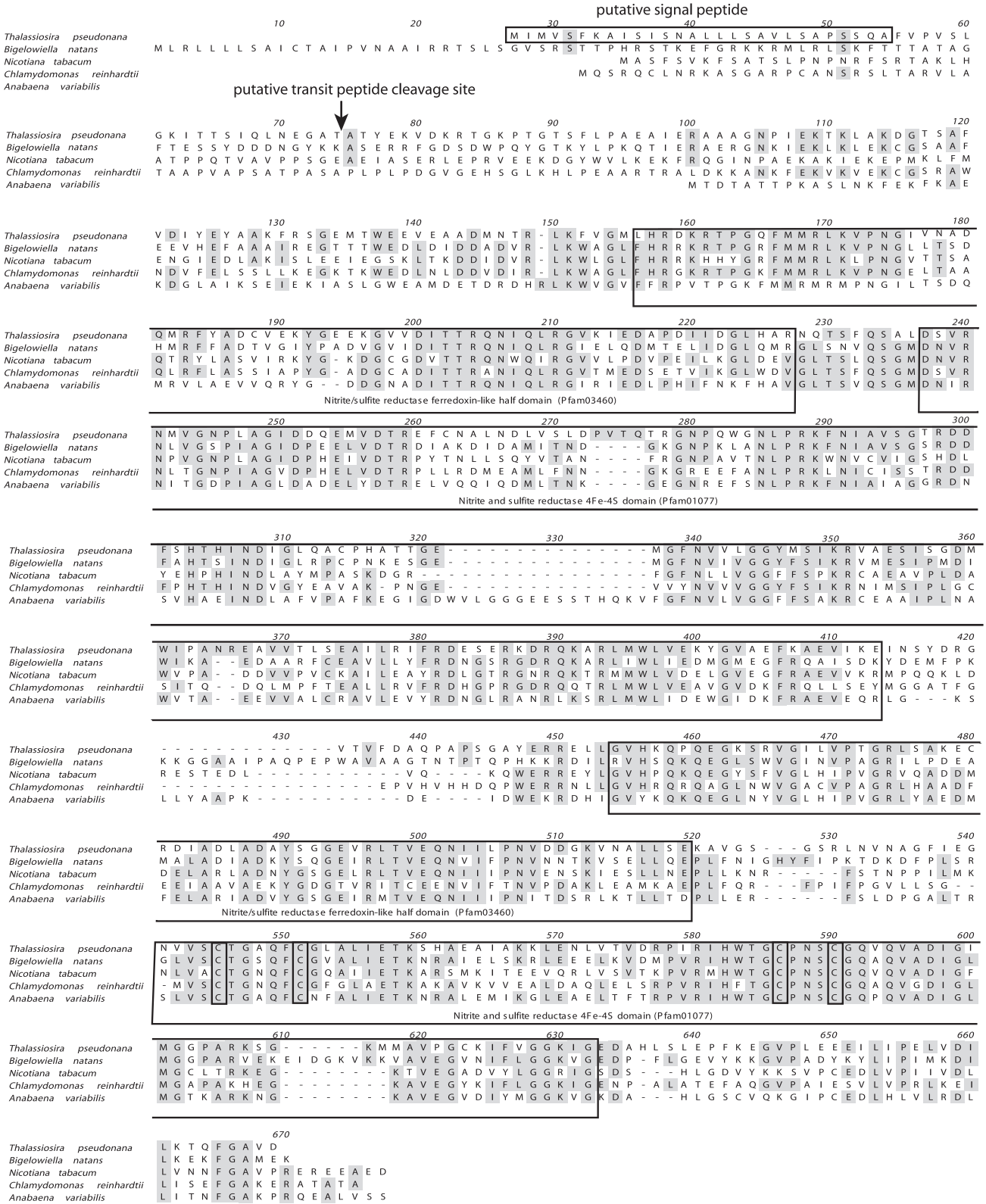

FIG. 3. Amino acid alignment of Fd-dependent NiR from the diatom *Thalassiosira pseudonana* (Protein ID 26941), the chlorarachniophyte *Bigelowiella natans* (GenBank accession AAP79144), the vascular plant *Nicotiana tabacum* (GenBank accession BAD15365), the green alga *Chlamydomonas reinhardtii* (GenBank accession CAA70137), and the cyanobacterium *Anabaena variabilis* ATCC 2941 (GenBank accession YP 325032). Numbering in the alignment is based on the *B. natans* sequence. Shaded residues represent amino acids that are identical to *T. pseudonana*. The putative signal and transit peptide sequences, conserved domains, and well-conserved cysteine residues (C) are boxed. Protein family (Pfam) identifiers are provided for each domain (http://pfam.sanger.ac.uk/).

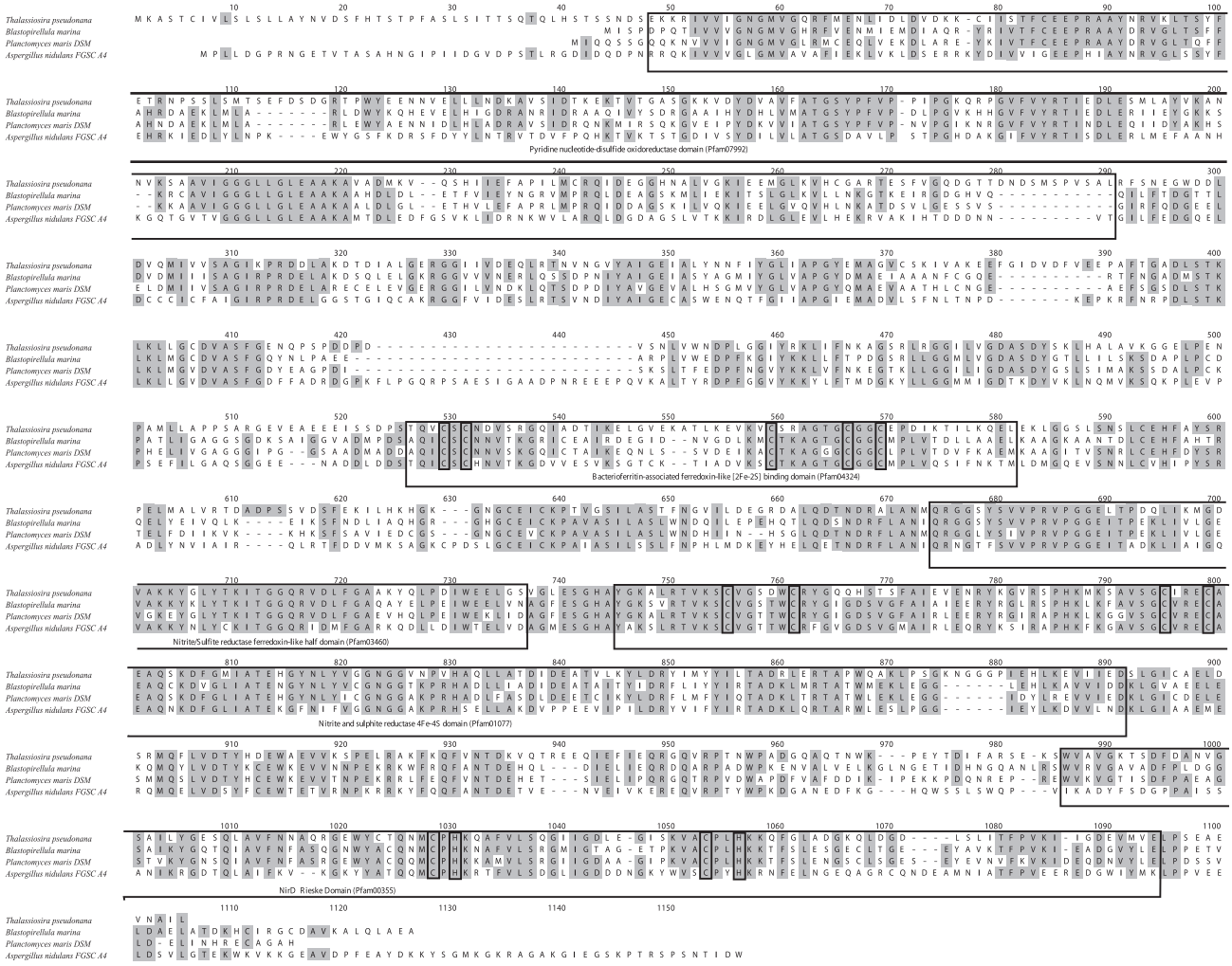

FIG. 4. Amino acid alignment of NAD(P)H-dependent NiR from the diatom *Thalassiosira pseudonana* (Protein ID 26941), the bacteria *Blastopirellula marina* DSM 3645 and *Planctomyces maris* DSM 8797 (GenBank accession ZP 01093337 and ZP 01854725, respectively), and the fungus *Aspergillus nidulans* FGSC A4 (GenBank accession XP 658611). Numbering in the alignment is based on the *T. pseudonana* sequence. Shaded residues represent amino acids that are identical to *T. pseudonana*. Conserved domains and well-conserved cysteine residues (C) are boxed. Protein family (Pfam) identifiers are provided for each domain (http://pfam.sanger.ac.uk/).

cleavage site for the signal peptide (Fig. 4) did not conform well with the diatom consensus sequence (''ASAFAP''; Kilian and Kroth 2005, Gruber et al. 2007). In addition, the length of the N-terminal region of fungal NAD(P)H-NiRs was variable (data not shown), and when aligned with fungal homologues, the N-terminal region of the *T. pseudonana* NAD(P)H-NiR protein was not significantly larger, as observed in the comparison of *Aspergillus nidulans* and *T. pseudonana* (Fig. 4). Thus, while further characterization will be required to determine the precise cellular location of the NAD(P)H-NiR, we favor the hypothesis that the enzyme functions in the cytoplasm of the diatom cell.

*Nir*B transcripts accumulated during the first 24 h following the transition to NO_3^--enriched seawater and were ~1,000 times more abundant at the onset of the second light period than at the time of the transition to new media (Fig. 2C). With the exception of the increase in transcript levels during the first light period, the diurnal oscillation of *nir*B transcript accumulation was out of phase from that of *nia* and *nii*A mRNA. *Nir*B mRNA abundance was high prior to or at the onset of the light period and decreased nearly 10-fold 6 h after the onset of the light before increasing during the later part of the light period.

Glutamine synthetases. Diurnal oscillations in mRNA levels were observed for both *gln*II and *gln*N (Fig. 2, D and E, respectively). For *gln*II, encoding the chloroplast localized GSII, there was a transient increase in transcript levels 2 h after the transfer to NO_3^--enriched media after which transcript levels remained low for the remainder of the light period.

Maximal transcript levels were measured prior to the onset of the second light period (22 h) and were approximately an order of magnitude more abundant than in the initial samples (0 h). Transcript levels declined following the onset of the light period, and minimal levels were measured 30 h from the transition to new media. Similarly, transcript levels were high at the onset of the third light period and decreased throughout the photoperiod.

*Gln*N transcript levels decreased approximately 10-fold 4 h into the first light period following the transition to NO_3^--enriched media before increasing throughout the remainder of the light period (Fig. 2E). The diurnal pattern of mRNA accumulation was similar during the next 2 d of the experiment, with daily maxima occurring near the onset of the light period and daily minima measured 2 h into the light phase. Transcript abundance was ~30-fold higher 24 h following the transfer of cells to NO_3^--enriched media, and by the end of the third light phase, transcripts levels were ~20 times greater than levels at the onset of the first light period (0 h).

Patterns of mRNA accumulation in response to L:D cycles and continuous irradiance. We investigated whether the diurnal oscillation in *nia* mRNA abundance was regulated by the circadian oscillator by entraining cells to a 12:12 L:D cycle and comparing *nia* accumulation to cells maintained on L:D (Fig. 5A) with those shifted to continuous light (Fig. 5B). Transcript accumulation patterns of *nia* entrained and maintained on an L:D cycle were similar over the course of three light periods and mirrored the pattern of *nia* oscillation observed on days 2 and 3 in the previous experiment (Fig. 2A). Transcript levels were the highest at the onset of the light phase, decreased ~10-fold over the course of the day, and increased over the dark period. The diurnal oscillation in *nia* transcript abundance was abolished after *T. pseudonana* cells were transferred to continuous light, indicating that the diurnal change in *nia* mRNA levels was not controlled by the circadian oscillator (Fig. 5B). There was no significant difference in the relative abundance of *nia* between the two treatments ($F_{1,2} = 6.5377$; $P = 0.1249$). However, there was a statistically significant treatment by time interaction ($F_{1,12} = 4.7327$; $P = 0.0006$), indicating that the pattern of *nia* accumulation was different in the cells grown on L:D and L:L, even though transcript abundance varied over time in both treatments (Table 3).

The diurnal oscillations observed in the expression of genes downstream in the nitrate assimilatory pathway (Fig. 6) were also abolished when cells were transferred to continuous light. As observed for *nia* accumulation, the diurnal variations in *nii*A, *nir*B, *gln*II, and *gln*N transcript levels in cells maintained on L:D were similar to those observed in Figure 2 (24–60 h). In contrast to cells maintained on L:D, transcript levels measured during the first photoperiod following the shift to L:L varied only slightly, indicating that diurnal changes in transcript accumulation for these four genes were not circadian controlled. The difference in the pattern of accumulation between the two treatments was most pronounced for *gln*II and *gln*N, as indicated by the statistically significant interaction term (Table 2). For all four genes (*nii*A, *nir*B, *gln*II, and *gln*N), transcript accumulation over the light period was more variable in cells grown on L:D than L:L (Table 3), consistent with the proposal that the diurnal oscillations were maintained L:D but not L:L.

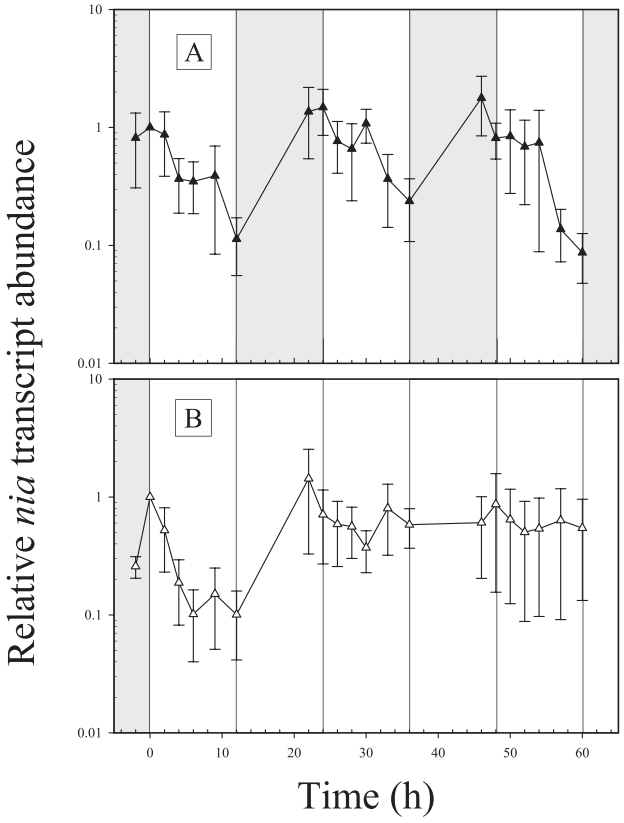

FIG. 5. Diurnal oscillations in *nia* mRNA accumulation were abolished when cells were transferred to continuous light (L:L), indicating that *nia* mRNA levels are not circadian controlled. Relative *nia* transcript levels are shown for cells maintained on a light:dark (L:D) cycle (A) as compared to those transferred to L:L (B) at $t = 0$ h. Shaded boxes represent the dark period. In both panels, symbols represent mean and ± 1 SE from three replicate cultures.

DISCUSSION

Field and laboratory studies of several algal species, including diatoms, have revealed a temporal lag between increases in nitrogen assimilation and increased growth rates, following a transition to improved growth conditions (Collos 1986, Duarte 1990, Dugdale et al. 1990). The temporal lag represents a period of metabolic adjustment and has

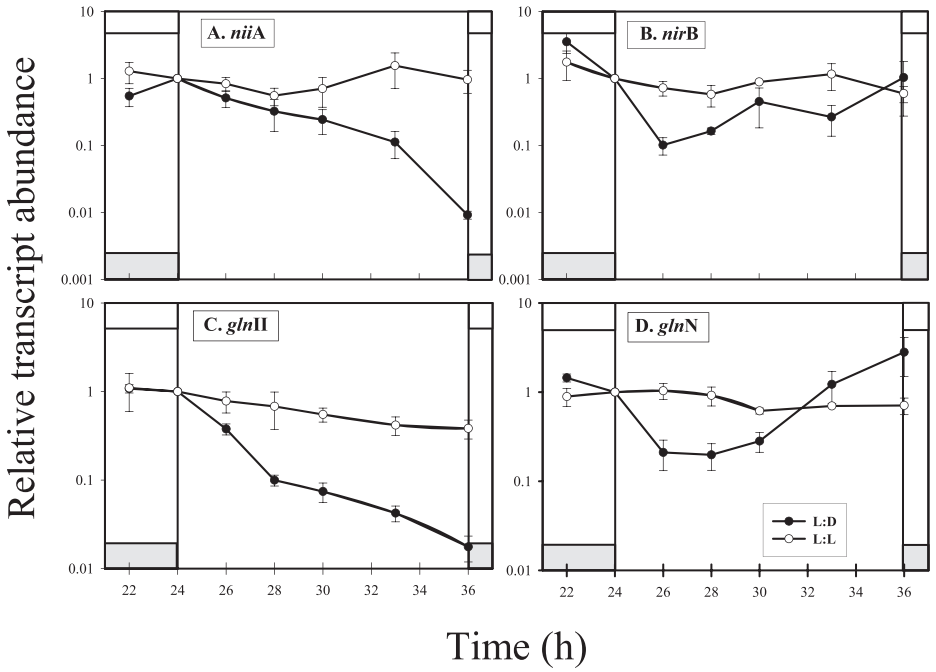

FIG. 6. Diurnal oscillations in *nii*A, *nir*B, *gln*II, *gln*N mRNA accumulation were abolished when cells were transferred to continuous light (L:L), indicating that mRNA levels were not circadian controlled. Experimental cultures (open circles) were switched from 12:12 L:D to L:L at $t = 24$ h. Dark circles represent cultures maintained on 12:12 L:D. Shaded boxes represent the dark period. In all panels, symbols represent mean and ± 1 SE from three replicate cultures.

TABLE 2. Multivariate analysis of variance (MANOVA) summary table analyzing patterns of transcript accumulation in cells maintained on L:D and L:L. Degrees of freedom (df) for the numerator and denominator, respectively, the calculated *F* value (*F*) and probability (*P*) are presented. Statistically significant *P* values are indicated (* $P < 0.05$).

Gene	Source	df	*F*	*P*
nia	Treatment	1, 2	6.5377	0.1249
	Time	12, 24	4.8904	0.0005*
	Treatment × time	12, 24	4.7327	0.0006*
*nii*A	Treatment	1, 2	3.1986	0.2158
	Time	5, 10	0.6504	0.6682
	Treatment × time	5, 10	1.1819	0.3830
*nir*B	Treatment	1, 2	0.0353	0.8682
	Time	5, 10	3.4764	0.0443*
	Treatment × time	5, 10	2.2404	0.1300
*gln*II	Treatment	1, 2	5.7163	0.1393
	Time	5, 10	22.9958	<0.0001*
	Treatment × time	5, 10	12.3865	0.0005*
*gln*N	Treatment	1, 2	0.1048	0.7769
	Time	5, 10	4.2442	0.0249*
	Treatment × Time	5, 10	5.6680	0.0098*

been used to examine the induction of specific enzyme systems and to identify cellular mechanisms regulating metabolic pathways (Smith et al. 1992, Huppe and Turpin 1994, Jochem et al. 2000). In this study, we identified temporal differences in the accumulation of mRNA of five genes involved in nitrogen assimilation in response to a transition in nitrogen availability and over the diel cycle. Transcript levels for the five genes studied here were greater in samples collected at the onset of the second light period than levels measured either before (−2 h) or at the transition to new media (0 h). The increase to near maximal levels 24 h following the transfer to improved growth conditions is consistent with an increase in nitrate assimilatory capacity.

The increase in *nia* mRNA levels in *T. pseudonana* cells following the transition to NO_3^--supplemented media was very similar to the temporal changes in NR protein abundance and activity observed in *Skeletonema costatum* following comparable transitions to improved growth conditions (Smith et al. 1992, Jochem et al. 2000). Although NR activity was barely detected in *S. costatum* during the first 24 h following the transition, NR abundance and activity increased during subsequent days and exhibited diel variation with maxima occurring near the middle of the light phase (Jochem et al. 2000), similar to the accumulation and the establishment of diurnal oscillations in *nia* levels in *T. pseudonana* reported here.

Diel periodicity in NR abundance and activity has also been reported for *T. pseudonana*, *T. weissflogii,* and natural assemblages of phytoplankton (Berges et al. 1995, Berges 1997, Vergara et al. 1998). As observed in *S. costatum*, NR abundance and activity have early to midday maxima, decreasing toward the end of the light period, and in some cases, a second peak of activity during the dark phase (Berges et al.

TABLE 3. Simple effects analyses examining variations in transcript accumulation in cells grown under L:D or L:L. Repeated measures multivariate analyses of variance (MANOVAs) were used to test the hypothesis there was significant variation in transcript accumulation over time. Degrees of freedom (df) and *F* as in Table 2. Statistically significant *P*-values are indicated [$*P < 0.025$ Bonferroni adjustment (Lehman et al. 2005); $**P < 0.05$].

Gene	Treatment	df	*F*	*P*
nia	L:D	12, 12	4.8105	0.0054*
	L:L	12, 12	4.8519	0.0052*
*nii*A	L:D	5, 5	6.1682	0.0337**
	L:L	5, 5	0.4895	0.7684
*nir*B	L:D	5, 5	3.0354	0.1242
	L:L	5, 5	0.7430	0.6238
*gln*II	L:D	5, 5	124.5578	<0.0001*
	L:L	5, 5	1.0429	0.4822
*gln*N	L:D	5, 5	5.3106	0.0454**
	L:L	5, 5	1.2170	0.4173

1995, Gao 1997). The diurnal variation of *nia* transcript accumulation measured in this study was similar to the variation in NR abundance and activity in studies of *T. pseudonana* and other diatoms with maxima in *nia* mRNA abundance proceeding maxima in enzyme abundance or activity. Thus, our results suggest that diurnal changes in transcript levels contribute, in part, to the observed changes in NR abundance and enzyme activity. Posttranscriptional, translational, or posttranslational processes may further modulate NR activity in diatoms.

Diel variations in transcripts levels were observed in the five genes examined in this study when cells were grown on L:D cycles but were abolished when cells were transferred to continuous light, indicating diurnal transcript accumulation is not circadian controlled. Similarly, Vergara et al. (1998) demonstrated that oscillations in NR abundance and activity were lost when *T. weissflogii* cells were transferred to continuous light. When grown on an L:D cycle, intracellular NO_3^- concentrations and N:C ratio in diatoms are high near the onset of the light period, decrease during the light phase, and then increase during the dark phase (Needoba and Harrison 2004), similar to our observed pattern of diurnal variation in *nia*, *nii*A, and *gln*II mRNA levels. Furthermore, oscillations in cellular N:C and intracellular NO_3^- are reduced or lost when cells are grown in continuous light (Gao 1997, Clark et al. 2002). Thus, as observed in prokaryotes, fungi, and vascular plants (Lancien et al. 2000, Palenchar et al. 2004), signaling pathways that sense changes in cellular nitrogen and carbon pools or metabolites may be important in the metabolic control of nitrogen assimilation in diatoms, including the regulation of gene expression. Alternatively, a signaling mechanism that responds to the redox status of the plastoquinone pool in chloroplasts has been linked to changes in NR expression and activity in *Chlamydomonas reinhardtii* (Giordano et al. 2005). A similar mechanism could be involved in regulating the diurnal changes in mRNA abundances observed in this study.

The phase of the diurnal variation in mRNA levels of the cytosolic-localized *nir*B and *gln*N was similar to each other but differed from that of *nia*, *nii*A, and *gln*II mRNA abundance. Minimal *nir*B and *gln*N transcript levels were observed early or mid-light phase, and transcript levels increased toward the end of the light period. This later increase in *nir*B and *gln*N mRNA levels may indicate a transition from chloroplastic- to cytoplasmic-localized nitrite reduction and ammonium assimilation and may contribute to the dark assimilation of nitrate observed in several species of diatoms (Berges et al. 1995, Clark et al. 2002, Needoba and Harrison 2004). Although nitrite is reduced in the dark in roots of vascular plants, the reaction is catalyzed by the plastid-localized ferredoxin-dependent NiR, which is reduced by NAD(P)H derived from the pentose phosphate pathway (Wray 1993, Swamy et al. 2005). In the diatoms, the NAD(P)H-dependent NiR may use reductant generated from the catabolism of carbon stores in the cytoplasm (Kroth et al. 2008). This hypothesis can be explored further by increasing sampling frequency during the dark phase coupled with measurements of enzyme activity.

Parker and Armbrust (2005) demonstrated that *gln*II mRNA abundance increased in response to increased rates of photorespiration in *T. pseudonana* grown under continuous illumination, implicating GSII in the assimilation of NH_4^+ produced by photorespiration. However, prior to this study, changes in *gln*N transcript levels in diatoms have not been reported. Recently, Roberts et al. (2007) showed that transcripts encoding phosphoenolpyruvate carboxylases (PEPC1 and PEPC2) and the P-subunit of glycine decarboxylase [GDCP], which are involved in generating carbon skeletons for NH_4^+ assimilation and photorespiration, were higher at the onset of the dark phase than at the beginning of the light period, suggesting increased rates of photorespiration occur in *T. pseudonana* near or at the end of the light phase. The increased accumulation of *gln*N mRNA toward the end of the light phase observed in our study may be correlated with the increased assimilation of photorespiratory-produced NH_4^+ in the cytoplasm of diatoms, in which case, the cytoplasmic localized GSIII may be involved with both the cytoplasmic assimilation of NO_3^- and NH_4^+ produced as a result of photorespiration.

Conclusions. We have documented the expression of five genes involved in the regulation of nitrogen assimilation in the marine diatom *T. pseudonana,* and our measurements of transcript levels provide insights into the regulation and coordination of nitrogen assimilation. The increase in *nia*, *nii*A, *nir*B, and *gln*II mRNA levels within 2 h of the transition to NO_3^--enriched media suggests the accumulation may be triggered by cellular fluxes in

nitrate. Following a period of acclimation (~24 h), diurnal patterns of mRNA accumulation were similar for enzymes involved in NO_3^- reduction and the chloroplast-localized reduction of NO_2^- and NH_4^+ assimilation (*nia*, *nii*A, and *gln*II). The diurnal oscillation of *nia*, *nii*A, and *gln*II was out of phase from that observed for *nir*B and *gln*N, a pathway that was heretofore unstudied in diatoms. Patterns of transcript accumulation support the hypothesis that *nir*B and *gln*N contribute to the dark assimilation of NO_3^- in diatoms, a hypothesis worthy of further biochemical exploration.

Little is known regarding the diurnal variation of Fd-NiR, NAD(P)H-NiR, GSII or GSIII abundance or activity; however, variations in *nia* abundance observed here were similar to those reported for NR abundance and activity in diatoms (Smith et al. 1992, Berges et al. 1995, Vergara et al. 1998, Jochem et al. 2000). Therefore, we propose the following model, on the basis of the assumption that mRNA levels are strong predictors of enzyme abundance and activity.

We propose that during the early light period, NO_3^- is rapidly assimilated via NR, Fd-NiR, and GSII. As proposed for vascular plants and green algae, flux in the cytosolic NO_3^- pool may be an important signal that coordinates patterns of gene expression (Stitt et al. 2002). Later in the light period, the chloroplastic reduction of NO_2^- declines, while cytosolic reduction of NO_2^- increases. The decline in chloroplast activity may be triggered by alterations in redox state, changes in pH, or reduced availability of C-skeletons. These changes could stimulate a signal cascade that either reduces gene transcription or alters the stability of *nia*, *nii*A, and *gln*II mRNA. During the dark, if carbon stores are sufficient, NO_3^- reduction occurs in the cytoplasm via the activity of NR, NAD(P)H-NiR, and GSIII, the transcript levels of which increase later in the light phase. Both GSII and GSIII appear to be involved in the assimilation of photorespiratory NH_4^+, with GSIII contributing more toward the end of the light period. Increases in the intracellular concentration of NO_3^- or changes in carbon and nitrogen metabolite pools during the dark period may stimulate the accumulation of *nia*, *nii*A, and *gln*II, resulting in high transcript levels at the onset of the light phase.

Thus, while regulatory networks that coordinate activities in the mitochondria, chloroplast, and cytosol were established independently following primary and secondary endosymbiotic acquisition of plastids, photosynthetic eukaryotes appear to respond to similar signaling molecules (e.g., intracellular NO_3^-, changes in cellular metabolite pools, and redox poise). It is likely that signal transduction pathways that coordinate nitrogen and carbon assimilation in diatoms will include mechanisms conserved among the different lineages of photoautotrophs as well as novel components that evolved following the secondary endosymbiotic events.

We thank S. Ghoshroy, T. Livdahl, D. Thurlow, and J. Thackeray for thoughtful comments on various aspects of the work. T. Livdahl provided helpful suggestions regarding the statistical analyses presented here. We thank two anonymous reviewers for valuable comments that enhanced the quality and focus of this manuscript. This work was supported by a NSF CAREER Award (IBN 0238426) to D. L. R. and funds from Clark University.

Allen, A. E., Vardi, A. & Bowler, C. 2006. An ecological and evolutionary context for integrated nitrogen metabolism and related signaling pathways in marine diatoms. *Curr. Opin. Plant Biol.* 9:264–73.

Altschul, S. F., Madden, T. L., Schaffer, A. A., Zhang, J., Zhang, Z., Miller, W. & Lipman, D. J. 1997. Gapped BLAST and PSI-BLAST: a new generation of protein database search programs. *Nucleic Acid Res.* 25:3389–402.

Armbrust, E. V., Berges, J. A., Bowler, C., Green, B. R., Martinez, D., Putnam, N. H., Zhou, S., et al. 2004. The genome of the diatom *Thalassiosira pseudonana*: ecology, evolution, and metabolism. *Science* 306:79–86.

Berges, J. A. 1997. Algal nitrate reductase. *Eur. J. Phycol.* 32:3–8.

Berges, J. A., Cochlan, W. P. & Harrison, P. J. 1995. Laboratory and field responses of algal nitrate reductase to diel periodicity in irradiance, nitrate exhaustion, and the presence of ammonium. *Mar. Ecol. Prog. Ser.* 124:259–69.

Berges, J. A. & Harrison, P. J. 1995. Nitrate reductase activity quantitatively predicts the rate of nitrate incorporation under steady state light limitation: a revised assay and characterization of the enzyme in three species of phytoplankton. *Limnol. Oceanogr.* 40:82–93.

Blasing, O. E., Gibon, Y., Gunther, M., Hohne, M., Morcuende, R., Osuna, D., Thimm, O., Usadel, B., Scheible, W.-R. & Stitt, M. 2005. Sugars and circadian regulation make major contributions to the global regulation of diurnal gene expression in *Arabidopsis*. *Plant Cell.* 17:3257–81.

Bode, A., Botas, J. A. & Fernandez, E. 1997. Nitrate storage by phytoplankton in a coastal upwelling environment. *Mar. Biol.* 129:399–406.

Bruland, K. W., Rue, E. L., Smith, G. J. & DiTullio, G. R. 2005. Iron, macronutrients and diatom blooms in the Peru upwelling regime: brown and blue waters of Peru. *Mar. Chem.* 93:81–103.

Clark, D. R., Flynn, K. J. & Owens, N. J. P. 2002. The large capacity for dark nitrate-assimilation in diatoms may overcome nitrate limitation of growth. *J. Phycol.* 155:101–8.

Colandene, J. D. & Garrett, R. H. 1996. Functional dissection and site-directed mutagenesis of the structural gene for NAD(P)H-nitrite reductase in *Neurospora crassa*. *J. Biol. Chem.* 271:24096–104.

Collos, Y. 1986. Time-lag algal growth dynamics: biological constraints on primary production in aquatic environments. *Mar. Ecol. Prog. Ser.* 33:193–206.

Dickson, M. L. & Wheeler, P. A. 1995. Ammonium uptake and regeneration rates in a coastal upwelling regime. *Mar. Ecol. Prog. Ser.* 121:239–48.

Dortch, Q. 1990. The interaction between ammonium and nitrate uptake in phytoplankton. *Mar. Ecol. Prog. Ser.* 61:183–201.

Dortch, Q., Clayton, J. R., Thoresen, S. S. & Ahmed, S. I. 1984. Species differences in accumulation of nitrogen pools in phytoplankton. *Mar. Biol.* 81:237–50.

Duarte, C. M. 1990. Time lags in algal growth: generality, causes and consequences. *J. Plankton Res.* 12:873–83.

Dugdale, R. C., Wilkerson, F. P. & Morel, A. 1990. Realization of new production in coastal upwelling areas: a means to compare relative performance. *Limnol. Oceanogr.* 35:822–9.

Emanuelsson, O., Nielsen, H., Brunak, S. & von Heijne, G. 2000. Predicting subcellular localization of proteins based on their N-terminal amino acid sequence. *J. Mol. Biol.* 300:1005–16.

Emanuelsson, O., Nielsen, H. & von Heijne, G. 1999. ChloroP, a neural network-based method for predicting chloroplast transit peptides and their cleavage sites. *Protein Sci.* 8:978–84.

Foyer, C. H., Parry, M. & Noctor, G. 2003. Markers and signals associated with nitrogen assimilation in higher plants. *J. Exp. Bot.* 54:585–93.

Gao, Y. 1997. Nitrate assimilation: biochemical and environmental control. Ph.D. dissertation, Dept. of Biological Sciences, University of Southern California, Los Angeles, 200 pp.

Garg, R. P., Vargo, C. J., Cui, X. & Kurtz, D. M. 1996. A [2Fe–2S] protein encoded by an open reading frame upstream of the *Escherichia coli* bacterioferritin gene. *Biochemistry* 35:6297–301.

Giordano, M., Chen, Y.-B., Koblizek, M. & Falkowski, P. G. 2005. Regulation of nitrate reductase in *Chlamydomonas reinhardtii* by the redox state of the plastoquinone pool. *Eur. J. Phycol.* 40:345–52.

Gruber, A., Vugrinec, S., Hempel, F., Gould, S. B., Maier, U.-G. & Kroth, P. G. 2007. Protein targeting into complex diatom plastids: functional characterisation of a specific targeting motif. *Plant Mol. Biol.* 64:519–30.

Guillard, R. 1975. Culture of phytoplankton for feeding marine invertebrates. *In* Smith, W. & Chanley, M. [Eds.] *Culture of Marine Invertebrate Animals.* Plenum Press, New York, pp. 29–60.

Guillard, R. & Ryther, J. H. 1962. Studies of marine planktonic diatoms I. *Cyclotella nana* Hustedt and *Detonula confervacea* Cleve. *Can. J. Microbiol.* 8:229–39.

Hernandez-Lopez, J. & Vargas-Albores, F. 2003. A microplate technique to quantify nutrients (NO_2^-, NO_3^-, NH_4^+ and $PO^{3/4-}$) in seawater. *Aquac. Res.* 34:1201–4.

Hildebrand, M. 2005. Cloning and functional characterization of ammonium transporters from the marine diatom *Cylindrotheca fusiformis* (Bacillariophyceae). *J. Phycol.* 41:105–13.

Hildenbrand, M. & Dahlin, K. 2000. Nitrate transporter genes from the diatom *Cylindrotheca fusiformis* (Bacillariophyceae): mRNA levels controlled by nitrogen and during the cell cycle. *J. Phycol.* 36:702–13.

Hodges, M. 2002. Enzyme redundancy and the importance of 2-oxoglutarate in plant ammonium assimilation. *J. Exp. Bot.* 53:905–16.

Huppe, H. C. & Turpin, D. H. 1994. Integration of carbon and nitrogen metabolism in plant and algal cells. *Annu. Rev. Plant Physiol. Plant Mol. Biol.* 45:557–607.

Jochem, F. J., Smith, G. J., Gao, Y., Zimmerman, R. C., Cabello-Pasini, A., Kohrs, D. G. & Alberte, R. S. 2000. Cytometric quantification of nitrate reductase by immunolabeling in the marine diatom *Skeletonema costatum. Cytometry* 3:173–8.

Jones, M. N. 1984. Nitrate reduction by shaking with cadmium: alternative to cadmium columns. *Water Res.* 18:643–6.

Kilian, O. & Kroth, P. G. 2005. Identification and characterization of a new conserved motif within the presequence of proteins targeted into complex diatom plastids. *Plant J.* 41:175–83.

Krishnamurthy, N., Brown, D., Kirshner, D. & Sjölander, K. 2006. PhyloFacts: an online structural phylogenomic encyclopedia for protein functional and structural classification. *Genome Biol.* 7:R83.

Kroth, P. G., Chiovitti, A., Gruber, A., Martin-Jezequel, V., Mock, T., Parker, M. S., Stanley, M. S., et al. 2008. A model for carbohydrate metabolism in the diatom *Phaeodactylum tricornutum* deduced from comparative whole genome analysis. *PLoS ONE* 3:e1426.

Kudela, R. M., Cochlan, W. P. & Dugdale, R. C. 1997. Carbon and nitrogen uptake response to light by phytoplankton during an upwelling event. *J. Plankton Res.* 19:609–30.

Kudela, R. M. & Dugdale, R. C. 2000. Nutrient regulation of phytoplankton productivity in Monterey Bay, California. *Deep-Sea Res. Part II.* 47:1023–53.

Lam, H.-M., Coschigano, K. T., Oliveira, I. C., Melo-Oliveira, R. & Coruzzi, G. M. 1996. The molecular-genetics of nitrogen assimilation into amino acids in higher plants. *Annu. Rev. Plant Physiol. Mol. Biol.* 47:569–93.

Lancien, M., Gadal, P. & Hodges, M. 2000. Enzyme redundancy and the importance of 2-oxoglutarate in higher plant ammonium assimilation. *Plant Physiol.* 123:817–24.

Lea, P. J. 1993. Nitrogen metabolism. *In* Lea, P. J. & Leegood, R. C. [Eds.] *Plant Biochemistry and Molecular Biology.* John Wiley and Sons, New York, pp. 312.

Lehman, A., O'Rouke, N., Hatcher, L. & Stepanski, E. J. 2005. *JMP for Basic Univariate and Multivariate Statistics: A Step-by-Step Guide.* SAS Institute Inc., Cary, North Carolina, 481 pp.

Lillo, C., Meyer, C. & Ruoff, P. 2001. The nitrate reductase circadian system. The central clock dogma contra multiple oscillatory feedback loops. *Plant Physiol.* 125:1554–7.

Livak, K. J. & Schmittgen, T. D. 2001. Analysis of relative gene expression data using real-time quantitative PCR and the $2^{-\Delta\Delta Ct}$ method. *Methods* 25:402–8.

Lomas, M. W. & Glibert, P. M. 1999a. Temperature regulation of nitrate uptake: a novel hypothesis about nitrate uptake and reduction in cool-water diatoms. *Limnol. Oceanogr.* 44:556–72.

Lomas, M. W. & Glibert, P. M. 1999b. Interactions between NH_4^+ and NO_3^- uptake and assimilation: comparison of diatoms and dinoflagellates at several growth temperatures. *Mar. Biol.* 133:541–51.

Luu-The, V., Paquet, N., Calvo, E. & Cumps, J. 2005. Improved real-time RT-PCR method for high-throughput measurements using second derivative calculation and double correction. *BioTechniques* 38:297–3.

Marchler-Baue, A., Anderson, J., Derbyshire, M., DeWeese-Scott, C., Gonzales, N., Gwadz, M., Hao, L. et al. 2007. CDD: a conserved domain database for interactive domain family analysis. *Nucleic Acids Res.* 35:D237–40.

Milligan, A. J. & Harrison, P. J. 2000. Effects on non-steady-state iron limitation on nitrogen assimilatory enzymes in the marine diatom *Thalassiosira weissflogii* (Bacillariophyceae). *J. Phycol.* 36:78–86.

Needoba, J. A. & Harrison, P. J. 2004. Influence of low light and a light:dark cycle on NO_3^- uptake, intracellular NO_3^- and nitrogen isotope fractionation by marine phytoplankton. *J. Phycol.* 40:505–16.

Nielsen, H., Engelbrecht, J., Brunak, S. & von Heijne, G. 1997. Identification of prokaryotic and eukaryotic signal peptides and prediction of their cleavage sites. *Protein Eng.* 10:1–6.

Olmo-Mira, M. F., Cabello, P., Pino, C., Martinez-Luque, M., Richardson, D. J., Castillo, F., Roldan, M. D. & Moreno-Vivian, C. 2006. Expression and characterization of the assimilatory NADH-nitrite reductase from the phototrophic bacterium *Rhodobacter capsulatus* E1F1. *Arch. Microbiol.* 186:339–44.

Palenchar, P., Kouranov, A., Lejay, L. & Coruzzi, G. 2004. Genome-wide patterns of carbon and nitrogen regulation of gene expression validate the combined carbon and nitrogen (CN)-signaling hypothesis in plants. *Genome Biol.* 5:R91.

Parker, M. S. & Armbrust, E. V. 2005. Synergistic effects of light, temperature and nitrogen source on transcription of genes for carbon and nitrogen metabolism in the centric diatom *Thalassiosira pseudonana* (Bacillariophyceae). *J. Phycol.* 41:1142–53.

Parsons, T. R., Maita, Y. & Lalli, C. M. 1984. *A Manual of Chemical and Biological Methods for Seawater Analysis.* Pergamon Press, New York, 173 pp.

Poulsen, N., Chesley, P. M. & Kröger, N. 2006. Molecular genetic manipulation of the diatom *Thalassiosira pseudonana* (Bacillariophyceae). *J. Phycol.* 42:1059–65.

Poulsen, N. & Kroger, N. 2005. A new molecular tool for transgenic diatoms. Control of mRNA and protein biosynthesis by an inducible promoter-terminator cassette. *FEBS J.* 272:7413–23.

Roberts, K., Granum, E., Leegood, R. C. & Raven, J. A. 2007. C3 and C4 pathways of photosynthetic carbon assimilation in marine diatoms are under genetic, not environmental, control. *Plant Physiol.* 145:230–45.

Robertson, D. L. & Alberte, R. S. 1996. Isolation and characterization of glutamine synthetase from the marine diatom *Skeletonema costatum. Plant Physiol.* 111:1169–75.

Robertson, D. L., Smith, G. J. & Alberte, R. S. 1999. Characterization of a cDNA encoding glutamine synthetase from the marine diatom *Skeletonema costatum* (Bacillariophyceae). *J. Phycol.* 35:786–97.

Sambrook, J. & Russell, D. 2001. *Molecular Cloning: A Laboratory Manual.* 3rd ed. Cold Spring Harbor Laboratory Press, Cold Spring Harbor, New York, 999 pp.

Scheible, W.-R., Morcuende, R., Czechowski, T., Fritz, C., Osuna, D., Palacios-Rojas, N., Schindelasch, D., Thimm, O., Udvardi, M. K.

& Stitt, M. 2004. Genome-wide reprogramming of primary and secondary metabolism, protein synthesis, cellular growth processes, and the regulatory infrastructure of *Arabidopsis* in response to nitrogen. *Plant Physiol.* 136:2483–99.

Smith, G. J., Zimmerman, R. C. & Alberte, R. S. 1992. Molecular and physiological responses of diatoms to variable levels of irradiance and nitrogen availability: growth of *Skeletonema costatum* in simulated upwelling conditions. *Limnol. Oceanogr.* 37:989–1007.

Stitt, M. 1999. Nitrate regulation of metabolism and growth. *Curr. Opin. Plant Biol.* 2:178–86.

Stitt, M., Muller, C., Matt, P., Gibon, Y., Carillo, P., Morcuende, R., Scheible, W.-R. & Krapp, A. 2002. Steps towards an integrated view of nitrogen metabolism. *J. Exp. Bot.* 53:959–70.

Swamy, U., Wang, M., Tripathy, J. N., Kim, S.-K., Hirasawa, M., Knaff, D. B. & Allen, J. P. 2005. Structure of spinach nitrite reductase: implications for multi-electron reactions by the iron–sulfur:siroheme cofactor. *Biochemistry* 44:16054–63.

Takabayashi, M., Wilkerson, F. P. & Robertson, D. L. 2004. Response of glutamine synthetase gene transcription and enzyme activity to external nitrogen sources in the diatom *Skeletonema costatum* (Bacillariophyceae). *J. Phycol.* 41:84–94.

Thompson, J. D., Higgins, D. G. & Gibson, T. J. 1994. Clustal W: improving the sensitivity of progressive multiple sequence alignment through sequence weighting, positions-specific gap penalties and weight matrix choice. *Nucleic Acid Res.* 22:4673–80.

Turpin, D. H. 1991. Effects of inorganic N availability on algal photosynthesis and carbon metabolism. *J. Phycol.* 27:14–20.

Vergara, J. J., Berges, J. A. & Falkowski, P. G. 1998. Diel periodicity of nitrate reductase activity and protein levels in the marine diatom *Thalassiorsira weissflogii* (Bacillariophyceae). *J. Phycol.* 34:952–61.

Wang, R., Guegler, K., LaBrie, S. T. & Crawford, N. M. 2000. Genomic analysis of a nutrient response in *Arabidopsis* reveals diverse expression patterns and novel metabolic and potential regulatory genes induced by nitrate. *Plant Cell.* 12:1491–510.

Wilkerson, F. P., Dugdale, R. C., Kudela, R. M. & Chavez, F. P. 2000. Biomass and productivity in Monterey Bay, California: contribution of the large phytoplankton. *Deep-Sea Res. Part II.* 47:1003–22.

Wray, J. L. 1993. Molecular biology, genetics and regulation of nitrite reductase in higher plants. *Physiol. Plant.* 89:607–12.

Zehr, J. P. & Falkowski, P. G. 1988. Pathway of ammonium assimilation in a marine diatom determined with the radiotracer ^{13}N. *J. Phycol.* 24:588–91.